SUPPORTING INFORMATION

SHG–active Ln^{III}–$[Mo^I(CN)_5(NO)]^{3-}$ (Ln = Gd, Eu) magnetic coordination chains: a new route towards non-centrosymmetric molecule-based magnets

Masaya Komine,[a] Szymon Chorazy,[a,b] Kenta Imoto,[a] Koji Nakabayashi,[a] and Shin-ichi Ohkoshi[a]*

[a]*Department of Chemistry, School of Science, The University of Tokyo, 7-3-1 Hongo, Bunkyo-ku, Tokyo, 113-0033, Japan.*
[b]*Faculty of Chemistry, Jagiellonian University, Ingardena 3, 30-060 Krakow, Poland.*

*Corresponding authors: ohkoshi@chem.s.u-tokyo.ac.jp

Experimental details.

Materials

Europium(III) chloride hexahydrate (CAS: 15759-92-7), gadolinium(III) nitrate hexahydrate (CAS: 19598-90-4), and N,N'-dimethylformamide (dmf, CAS: 68-12-2) were purchased from Wako Pure Chemical Industries, Ltd., and used without further purification. The heteroligand pentacyanidonitrosylmolybdate(I) precursor in the form of $(PPh_4)_3[Mo^I(CN)_5(NO)]\cdot2H_2O$ (PPh$_4$ = tetraphenylphosphonium) salt was prepared following the literature method.[S1]

Synthesis and basic characterization of 1

The synthesis of **1** was conducted under an argon atmosphere due to the sensitivity of the cyanide precursor and the final product to the exposition to an air atmosphere. $Gd^{III}(NO_3)_3\cdot6H_2O$ (0.01 mmol, 4.5 mg) was dissolved in 2 mL of dmf to prepare solution A, and $(PPh_4)_3[Mo^I(CN)_5(NO)]\cdot2H_2O$ (0.01 mmol, 13.1 mg) was dissolved in 2 mL of dmf to obtain solution B. Then, solution B was slowly added to solution A, and the mixed solution was left for crystallization for several days. After that, the yellowish green crystals were obtained, collected by a suction filtration, and washed with dmf. The resulting crystalline material was only fairly stable on the air, thus it was stored under an Ar atmosphere. The composition of $[Gd^{III}(dmf)_6][Mo^I(CN)_5(NO)]$ (**1**) was determined by the CHN elemental analysis of the standard microanalytical method, and the metal analysis executed by means of inductively coupled plasma mass spectrometry (ICP-MS) technique. Yield: 7.0 mg (83%). IR spectrum (nujol, CaF$_2$, cm^{-1}). CN$^-$ stretching vibrations: 2117, 2091, 2078. Elemental analysis. Anal. Calcd. for $Gd_1Mo_1C_{23}N_{12}O_7H_{42}$: Gd, 18.5%; Mo, 11.3%; C, 32.4%; H, 5.0%; N, 19.7%. Found: Gd, 18.5%; Mo, 11.4%; C, 32.6%; H, 5.0%; N, 19.9%.

Synthesis and basic characterization of 2

The synthetic procedure was conducted as described for **1**, but using $Eu^{III}(NO_3)_3\cdot6H_2O$ (0.01 mmol, 4.4 mg) instead of $Gd^{III}(NO_3)_3\cdot6H_2O$. Yellowish green crystals of **2** appeared after several days of crystallization. They were collected by suction filtration and washed with dmf. The resulting crystalline material was only fairly stable on the air, thus it was stored under an Ar atmosphere. The composition of $[Eu^{III}(dmf)_6][Mo^I(CN)_5(NO)]$ (**2**) was found the CHN and metal elemental analysis. Yield: 6.7 mg (79%). IR spectrum (nujol, CaF$_2$, cm^{-1}). CN$^-$ stretching vibrations: 2115, 2091, 2076. Elemental analysis. Anal. Calcd. for $Eu_1Mo_1C_{23}N_{12}O_7H_{42}$: Eu, 18.0%; Mo, 11.3%; C, 32.6%; H, 5.0%; N, 19.9%. Found: Eu, 18.0%; Mo, 11.4%; C, 32.4%; H, 5.0%; N, 19.8%.

Crystal structure determination

Single crystal X-ray diffraction analyses of **1** and **2** were performed using a Rigaku R-AXIS RAPID imaging plate area detector with graphite monochromated Mo Kα radiation. The single crystals were dispersed in a paratone-N oil, mounted on Micro Mounts^{TM} holder, and measured at the low temperature of 90(2) K. The intensity data were integrated by Rigaku RAPID AUTO. The crystal structures were solved by a direct method using SHELXS-97, and refined using a full-matrix least squares technique of SHELXL-2014/7.[S2] Calculations were executed using

partially Crystal Structure crystallographic software package, and partially WinGX (ver. 1.80.05) integrated system. Non hydrogen atoms were refined by using anisotropic atomic displacement parameter. Hydrogen atoms are placed at calculated positions and refined using a riding model. Structural diagrams were prepared using Mercury 3.5.1 programme. CCDC reference numbers for the crystal structures of **1** and **2** are 1508559 and 1508558, respectively. The details of the crystal structures and structure refinements are gathered in Table 1, while the selected structure parameters are presented in Table S1. The graphical presentations of the representative parts of the crystals structures of **1** and **2** are shown in Figures 1 and S2, respectively.

Physical techniques

Elemental analysis was performed by the standard micro analysis and Agilent 7700 inductively coupled plasma mass spectrometer (ICP-MS). Infrared absorption spectra were recorded with a JASCO IRT-3100 FT-IR microscope. Magnetic measurements were performed using a Quantum Design MPMS 5S on the polycrystalline sample protected by mother liquid and methyl methacrylate polymer (PMMA). The diamagnetic contribution from the holder, solution and the sample was estimated and subtracted from the raw data.

Powder X-ray diffraction patterns of the polycrystalline samples of **1** and **2** were collected on a Rigaku Ultima-IV equipped with CuKα radiation ($\lambda = 1.5418$ Å). For this measurements, the single crystals of **1** and **2** were grinded under Ar atmosphere, and packed into the sample holder, which was filled by inert gas and closed. Thus, the powder XRD experiments were performed without contact of the samples with the air. The powder diffractogramms of **1** and **2** are presented in Figure S3.

The setup of second harmonic generation (SHG) measurement is shown in Figure S1. The fundamental light is the idler light ($\lambda = 1064$ nm) of optical parametric amplifier (Clark-MXR vis-OPA), which is obtained by conversion of pump light ($\lambda = 775$ nm) from Ti:Sapphire laser (Clark-MXR CPA-2001). The focused fundamental light was passed through visible light cut filter to remove second harmonic light and irradiated to the sample with an incident angle of 90°. The reflected light was focused, passed through two IR cut filters, THG cut filter, and a band pass filter (532±10 nm), and guided to the photomultiplier tube (Hamamatsu R329-02).[S3]

Calculations

Continuous Shape Measure Analysis for the determination of the geometry of eight-coordinated Gd^{III} and Eu^{III} complexes was performed using a SHAPE software ver. 2.1.[S4] The results are presented in Table S2.
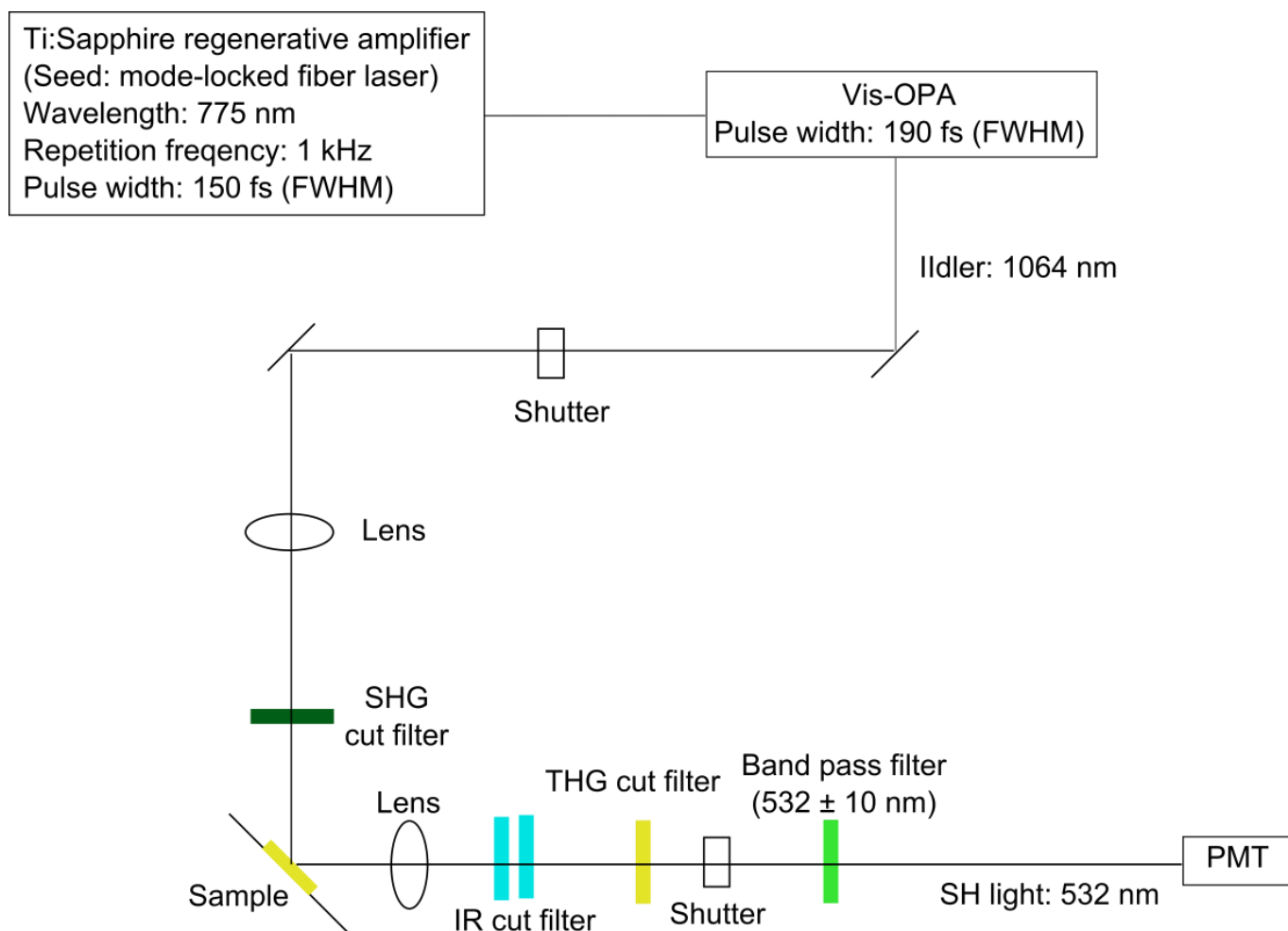
Figure S1. The experimental setup for the SHG measurement of the polycrystalline sample of **1**.

Table S1. Detailed structure parameters of **1** and **2**.

Details of [Mo^I(CN)$_5$(NO)]$^{3-}$ complexes			Details of [Ln^{III}(dmf)$_6$(NC)$_2$]$^+$ complexes		
Parameter	**1**	**2**	Parameter	**1** (Ln = Gd)	**2** (Ln = Eu)
Mo1 – C1	2.179(8) Å	2.178(9) Å	Ln1 – N1	2.487(6) Å	2.500(7) Å
Mo1 – C2	2.173(8) Å	2.174(8) Å	Ln1 – N2	2.509(7) Å	2.520(7) Å
Mo1 – C3	2.129(10) Å	2.138(11) Å	Ln1 – O2	2.399(6) Å	2.411(6) Å
Mo1 – C4	2.166(9) Å	2.161(10) Å	Ln1 – O3	2.378(6) Å	2.389(7) Å
Mo1 – C5	2.184(13) Å	2.197(13) Å	Ln1 – O4	2.388(5) Å	2.401(5) Å
Mo1 – N6	1.935(8) Å	1.928(9) Å	Ln1 – O5	2.418(7) Å	2.437(8) Å
C1 – N1	1.156(10) Å	1.156(11) Å	Ln1 – O6	2.336(7) Å	2.348(8) Å
C2 – N2	1.159(10) Å	1.158(11) Å	Ln1 – O7	2.392(6) Å	2.400(7) Å
C3 – N3	1.160(13) Å	1.154(14) Å	N1 – Ln1 – N2	138.3(2)°	138.2(2)°
C4 – N4	1.176(12) Å	1.177(13) Å	O2 – Ln1 – O3	79.9(2)°	79.1(2)°
C5 – N5	1.173(15) Å	1.154(16) Å	O5 – Ln1 – O6	81.2(2)°	81.5(2)°
N6 – O1	1.173(11) Å	1.183(12) Å	O4 – Ln1 – O7	78.0(2)°	78.0(2)°
Mo1 – C1 – N1	175.5(11)°	175.6(11)°	O6 – Ln1 – O7	72.7(2)°	72.7(3)°
Mo1 – C2 – N2	178.9(8)°	178.8(8)°	O4 – Ln1 – O5	70.8(2)°	71.0(2)°
Mo1 – C3 – N3	177.0(8)°	177.0(9)°	O2 – Ln1 – O6	109.3(2)°	109.0(3)°
Mo1 – C4 – N4	177.1(8)°	176.4(8)°	O2 – Ln1 – O7	73.0(2)°	72.8(2)°
Mo1 – C5 – N5	177.9(10)°	177.8(10)°	O3 – Ln1 – O4	111.1(2)°	111.1(3)°
Mo1 – N6 – O1	176.7(8)°	176.9(9)°	O3 – Ln1 – O5	74.2(2)°	74.4(2)°
C1 – Mo1 – C2	170.9(3)°	170.8(3)°	N1 – Ln1 – O7	119.0(3)°	119.3(3)°
C3 – Mo1 – C5	176.3(4)°	176.3(4)°	C1 – N1 – Ln1	171.2(6)°	171.2(7)°
C4 – Mo1 – N6	173.8(4)°	174.1(4)°	C2 – N2 – Ln1	164.3(7)°	164.1(7)°

Table S2. Results of Continuous Shape Measure Analysis for $[Ln^{III}(dmf)_6(NC)_2]^+$ complexes in **1** and **2**

Ln complex	CSM parameters			Geometry
	BTP-8	SAPR-8	DD-8	
$[Gd^{III}(dmf)_6(NC)_2]^+$, **1**	1.844	0.350	1.785	SAPR-8
$[Eu^{III}(dmf)_6(NC)_2]^+$, **1**	1.801	0.363	1.768	SAPR-8

* CSM parameters:[S4]

CSM BTP-8 = the parameter related to the bicapped trigonal prism geometry (C_{2v} symmetry)

CSM SAPR-8 = the parameter related to the square antiprism (D_{4d} symmetry)

CSM DD-8 = the parameter related to the dodecahedron (D_{2d} symmetry)

CSM = 0 for the ideal geometry and the increase of CSM parameter corresponds to the increasing distortion from the ideal polyhedron.
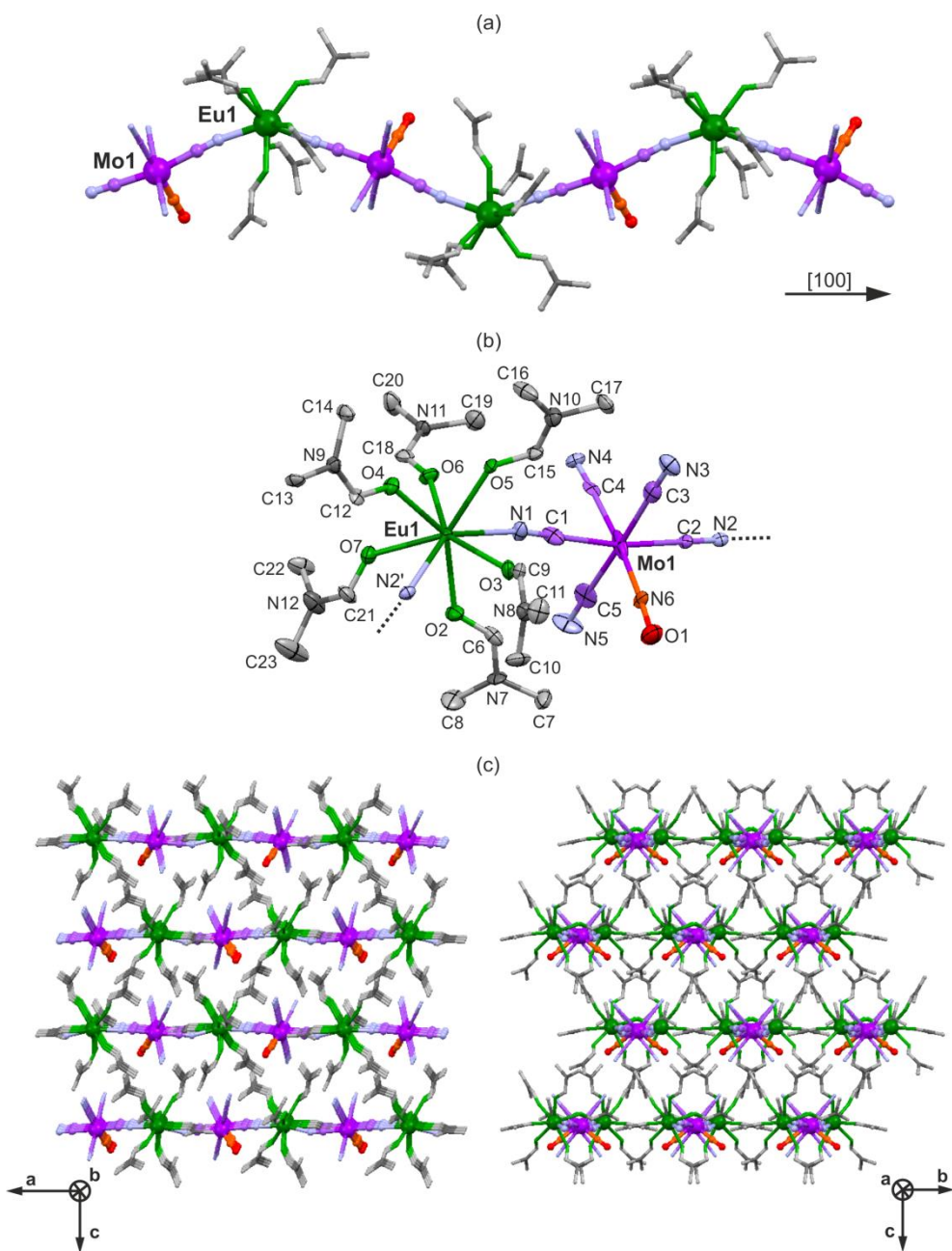
Figure S2. Crystal structure of **2**: (a) the representative fragment of coordination polymer, (b) asymmetric unit with the atoms shown at the 70% probability level with the atoms labelling scheme, and (c) the views of supramolecular arrangement of chains within the *ac* and *bc* planes.
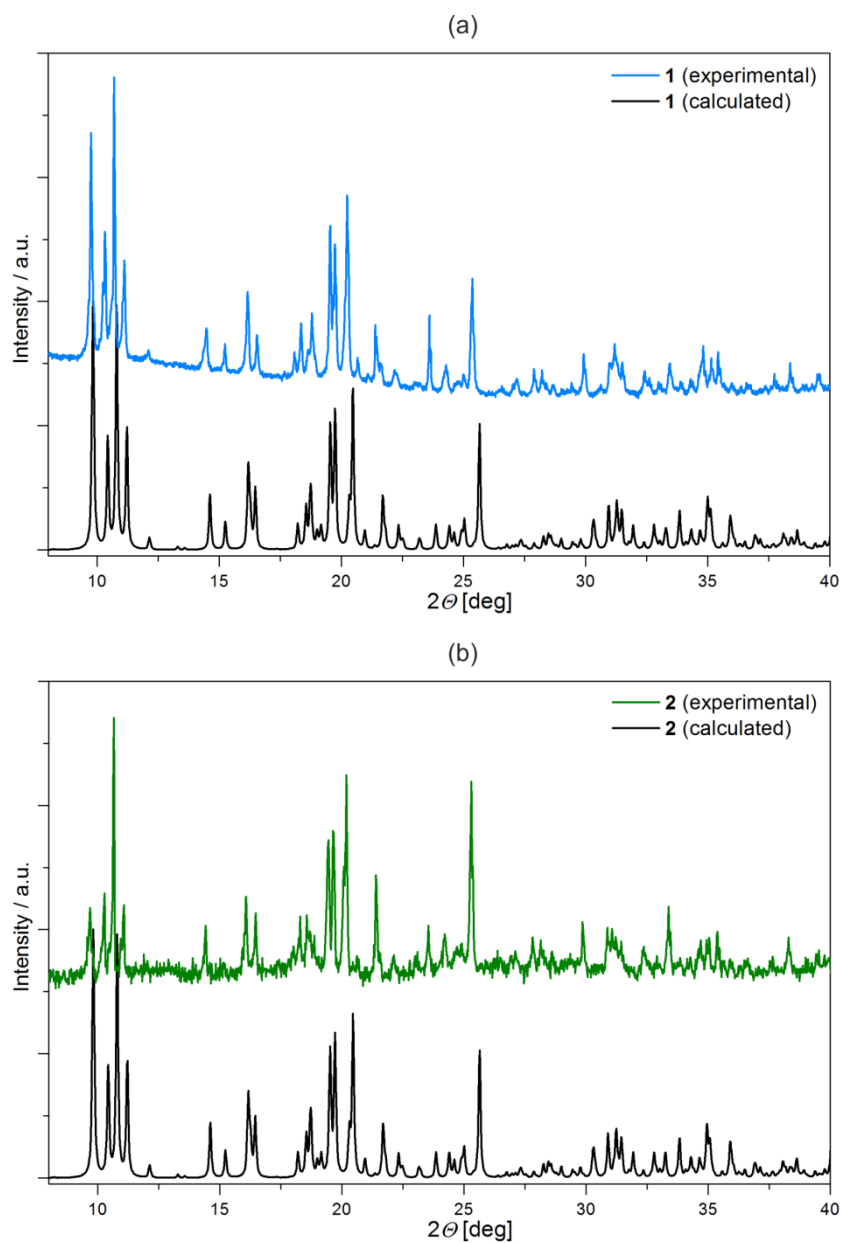
Figure S3. Experimental powder X-ray diffraction patterns of **1** (a) and **2** (b), compared with the respective calculated patterns based on the single-crystal XRD structural models (black lines).

Details of simulation of magnetic curve for 1

The $\chi_M T$ versus T plot of **1**, containing the magnetic Gd^{III} ($S_{Gd} = 7/2$) and Mo^I ($S_{Mo} = 1/2$) spin centers, was simulated using a Seiden's model for a spin alternating chain, in which one of the spins is sufficiently large (Gd^{III}) to be treated as a classical vector while the second (Mo^I) is small, and it is treated as a quantum spin.[S5]

In this model, the spin Hamiltonian with an exchange interaction (J_{exc}) is defined as

$$\hat{H} = -2J_{exc} \sum (S_{2i-1}^{Gd} + S_{2i+1}^{Gd}) S_{2i}^{Mo} \tag{1}$$

Following this spin Hamiltonian, after the rigorous mathematical calculation, we obtain the exact equation for the magnetic susceptibility of such a spin alternating chain built of Gd^{III} with spin S_{Gd}, the g-value g_{Gd} and Mo^I with spin S_{Mo}, the g-value g_{Mo}:[S5]

$$\chi_{M,calc} = \left(\frac{N\beta^2}{3}\right) \times \left[g_{Gd}^2 S_{Gd}^2 \left(\frac{S_{Gd}+1}{S_{Gd}} + \frac{2\delta}{1-\delta}\right) - \frac{4g_{Gd}g_{Mo}\Delta S_{Mo}S_{Gd}}{1-\delta} + g_{Mo}^2 \left(S_{Mo}(S_{Mo}+1) + \frac{2\Delta^2 S_{Mo}^2}{1-\delta}\right)\right] \tag{2}$$

where

$$\delta = \frac{A_1}{3A_0} \tag{2a}$$

$$\Delta = 2\left(\frac{B_1}{3A_0} + \frac{B_0}{A_0}\right) \tag{2b}$$

$$A_0 = 4(\gamma^{-1}\sinh\gamma - \gamma^{-2}\cosh\gamma + \gamma^{-2}) \tag{2c}$$

$$A_1 = 12[(\gamma^{-1} + 12\gamma^{-3})\sinh\gamma - (5\gamma^{-2} + 12\gamma^{-4})\cosh\gamma - \gamma^{-2} + 12\gamma^{-4}] \tag{2d}$$

$$B_0 = \gamma^{-1}(\cosh\gamma - 1) \tag{2e}$$

$$B_1 = 3(\gamma^{-1} + 4\gamma^{-3}\cosh\gamma - 4\gamma^{-2}\sinh\gamma + \gamma^{-1} - 4\gamma^{-3}) \tag{2f}$$

$$\gamma = -2\beta J_{exc}S_{Gd} \tag{2g}$$

$$\beta = \frac{1}{kT} \tag{2h}$$

Within the fitting procedure, we set the exchange coupling constant, J_{exc} and the spin value of Gd^{III}, S_{Gd} as the fitting parameters, taking the fixed g-value of Mo^I of 2.00, according to the ESR measurement.[S6]

The validity of the fitting procedure was checked by the R parameter defined by the equation:

$$R = \frac{\sum(\chi_{M,observed}T - \chi_{M,calculated}T)^2}{\sum \chi_{M,observed}T^2} \tag{3}$$

The best fit parameters (Fig. 2a, main text) are J_{exc} = -1.02(5) cm^{-1}, g_{Gd} = 2.01(1) with R = 0.016, indicating the successful fitting of the magnetic curve with the reasonable parameters as compared with the other reported bimetallic Gd-containing cyanido-bridged spin chain systems.[S6bc,S7]

Details of simulation of magnetic curve for 2

The $\chi_M T$ versus T plot of **2**, containing the magnetic Gd^{III} (S_{Gd} = 7/2) and Mo^I (S_{Mo} = 1/2) spin centers, was simulated taking into account the paramagnetism of Mo^I and the gradual thermal depopulation of the partially occupied excited states of Eu^{III} which generally reveals the diamagnetic $^7F_0$ ground state. The possible interactions between spin centers were not taken into account. Thus, the main role in the temperature dependence of the $\chi_M T$ product is played by the spin-orbit coupling effect on Eu^{III}. In general, the $^7F_0$ ground term of Eu^{III} is split by the spin-orbit coupling into seven states ^7F_J with J = 0, 1, 2, 3, 4, 5, 6. The spin orbit coupling operator reads H$_{SO}$ = $\lambda L \cdot S$, where λ is the spin-orbit coupling constant. Even that the ground state, $^7F_0$ is diamagnetic, the magnetic susceptibility of Eu^{III} is non-zero due to the partial thermal population of closely lying excited states with non-zero J values. The population of the excited states is controlled by the strength of the spin-orbit coupling splitting described by the λ value.[S8] Thus, the molar magnetic susceptibility of **2** may be expressed as the sum of the constant contribution from Mo^I (S_{Mo} = 1/2, g_{Mo} = 2.0, giving $\chi_M T$ = 0.375 cm^{3}mol^{-1}K), and the temperature-dependent contribution from Eu^{III} which is the function of T and λ:[S9]

$$\chi_{M,calc} = 0.375 + \frac{N\beta^2}{3kTx} \times \frac{A}{B} \tag{4}$$

where

$$A = 24 + \left(\frac{27x}{2} - \frac{3}{2}\right)e^{-x} + \left(\frac{135x}{2} - \frac{5}{2}\right)e^{-3x} + \left(189x - \frac{7}{2}\right)e^{-6x} + \left(405x - \frac{9}{2}\right)e^{-10x} + \left(\frac{1485x}{2} - \frac{11}{2}\right)e^{-15x} +$$

$$\left(\frac{2457x}{2} - \frac{13}{2}\right)e^{-21x} \tag{4a}$$

$$B = 1 + 3e^{-x} + 5e^{-3x} + 7e^{-6x} + 9e^{-10x} + 11e^{-15x} + 13e^{-21x} \tag{4b}$$

$$x = \lambda/kT \tag{4c}$$

The validity of the fitting procedure was checked by the R parameter defined by the equation (3) (see above).

The best fit with λ = 365(3) cm^{-1} and R = 0.18 (Fig. 2c, main text) well describes the experimental data. Thus, the magnetic centers of Eu^{III} and Mo^I can be treated as magnetically isolated, and the possible magnetic coupling between Mo^I spin centers through diamagnetic Eu^{III} can be neglected. The value of the obtained spin-orbit coupling constant of Eu^{III} is also reasonable among reported bimetallic Eu-based cyanido-bridged materials.[S7a,S9]

References to Supporting Information

[S1]   A. Müller, W. Eltzner, S. Sarkar, H. Bőgge, P. J. Aymonino, N. Mohan, U. Seyer and P. Subramanian, *Z. Anorg. Allg. Ch*em., 1983, **503**, 22.

[S2]   G. M. Sheldrick, *Acta Cryst*., 2008, **A64**, 112.

[S3]   T. Nuida, T. Matsuda, H. Tokoro, S. Sakurai, K. Hashimoto and S. Ohkoshi, *J. Am. Chem. Soc*., 2005, **127**, 11604.

[S4]   (a) M. Llunell, D. Casanova, J. Cirera, J. Bofill, P. Alemany, S. Alvarez, M. Pinsky and D. Avnir, *SHAPE ver. 2.1. Program for the Calculation of Continuous Shape Measures of Polygonal and Polyhedral Molecular Fragments*, University of Barcelona: Barcelona, Spain, 2013; (b) D. Casanova, J. Cirera, M. Llunell, P. Alemany, D. Avnir and S. Alvarez, *J. Am. Chem. Soc*., 2004, **126**, 1755.

[S5]   (a) J. Seiden, *J. Phys*., 1983, **44**, 947; (b) S. Ikeda, T. Hozumi, K. Hashimoto and S. Ohkoshi, *Dalton Trans*., 2005, 2120; (c) W. Kosaka, K. Hashimoto and S. Ohkoshi, *Bull. Chem. Soc. Jpn*., 2007, **80**, 2350.

[S6]   N. Machida, S. Ohkoshi, Z. J. Zhong and K. Hashimoto, *Chem. Lett*., 1999, 907.

[S7]   (a) P. Przychodzeń, R. Pełka, K. Lewiński, J. Supel, M. Rams, K. Tomala and B. Sieklucka, *Inorg. Chem*., 2007, **46**, 8924; (b) S. Chorazy, K. Nakabayashi, M. Arczynski, R. Pełka, S. Ohkoshi and B. Sieklucka, *Chem. Eur. J*., 2014, **20**, 7144.

[S8]   O. Kahn, *Molecular Magnetism*, VCH: New York, 1993.

[S9]   S. Chorazy, K. Nakabayashi, M. Ozaki, R. Pełka, T. Fic, J. Mlynarski, B. Sieklucka and S. Ohkoshi, *RSC Adv.*, 2013, **3**, 1065.